

Flexible circuits with integrated switches for robotic shape sensing

C. K. Harnett

Electrical and Computer Engineering Department, University of Louisville, 2210 S Brook St,
Louisville KY, USA 40208

ABSTRACT

Digital switches are commonly used for detecting surface contact and limb-position limits in robotics. The typical momentary-contact digital switch is a mechanical device made from metal springs, designed to connect with a rigid printed circuit board (PCB). However, flexible printed circuits are taking over from the rigid PCB in robotics because the circuits can bend while carrying signals and power through moving joints. This project is motivated by a previous work where an array of surface-mount momentary contact switches on a flexible circuit acted as an all-digital shape sensor compatible with the power resources of energy harvesting systems. Without a rigid segment, the smallest commercially-available surface-mount switches would detach from the flexible circuit after several bending cycles, sometimes violently. This report describes a low-cost, conductive fiber based method to integrate electromechanical switches into flexible circuits and other soft, bendable materials. Because the switches are digital (on/off), they differ from commercially-available continuous-valued bend/flex sensors. No amplification or analog-to-digital conversion is needed to read the signal, but the tradeoff is that the digital switches only give a threshold curvature value. Boundary conditions on the edges of the flexible circuit are key to setting the threshold curvature value for switching. This presentation will discuss threshold-setting, size scaling of the design, automation for inserting a digital switch into the flexible circuit fabrication process, and methods for reconstructing a shape from an array of digital switch states.

Keywords: compliant structure, conductive thread, bistable, digital switch, flexible circuits

1. INTRODUCTION

The movement toward flexible and stretchable electronics is motivated by the dynamic environments in robotics and wearable devices. Curved substrates and surfaces in constant motion are incompatible with the conventional rigid circuit board (PCB) format. Over the past ten years there has been a materials revolution in flexible and stretchable electronics, including ultrathin conventional materials with meandering traces [1], conductive liquid metal alloys [2,3] with applications in healthcare [4] and robotics [5], and knit conductive textiles [6]. The bulk of this materials-focused research is in the area of conductive traces [7], and passive devices such as antennas [8]. There have also been great advances in flexible batteries [9], temperature sensors [10], active-matrix sensor arrays [11], and displays [12,13]. However, there are still few flexible alternatives to mechanical connectors, motors, and switches.

Because these mechanical devices are essential to most robotics applications, there is already a technology base for integrating flexible printed circuits (flex-PCBs) with rigid components by inserting stiffeners in the thin polymer flex-PCB. Problems with the flex-rigid construction include stress concentration at the junctions, and the rigid segments' inability to conform to curved surfaces. In this work, we develop a new method to integrate conductive fibers with a flexible substrate, embedding a mechanical switch directly in the polymer sheet and eliminating the need for a rigid housing.

This paper presents a design for digital switches made by suspending conductive fibers over a gap that contains a moving cantilever cut from the bendable substrate. Because the end of the cantilever is unconstrained, it projects above or below the bending beam, creating a mechanical switch. We explore how to solve the problem of aligning a computer-embroidered pattern to a pre-cut design, and how to control the contact separation between the cantilever and the underlying material. Results are presented for buckling beams with different amounts of compression, and are discussed in the context of previous work with surface-mount switches as well as a multi-segment shape sensing application.

2. METHODOLOGY

2.1 Embroidery alignment with laser-cut parts

We are developing technology to incorporate a wide variety of fiber materials into 3D printed and laser-cut plastic parts. Because properties like tensile strength, crystal structure, and polymer alignment depend strongly on processing history, fibers cannot be 3D printed with the same properties they have on the spool. If they are used at all, technical fibers are installed by hand at the end of a fabrication sequence. Fabrication with advanced fiber materials is expensive, the materials are often not considered for high-volume manufacturing because of anticipated scaling problems, and then when a new fiber comes on the market, there is no well-worn path to bring it into production for robotics. The result is that the robotics community is not ready to take quick advantage of breakthroughs in fiber materials. Therefore, we are motivated to find computer-controlled fiber-integration methods that work with hard 3D printed, laser-cut and machined items.

Other groups have recognized the need for robotics- relevant materials beyond 3D printed plastic [14]. Fibers, especially cables and tendons, are critical in robotics and are an area where 3D printed materials can not compete. At the same time, computer-numerically-controlled (CNC) embroidery machines are available to consumers at extremely low price points (\$300 USD) with 10 x 10 cm patternable areas. While these machines are capable of 100 micron motion increments, they have limited alignment capability.

The machine used in this work, a Brother PE525 with a 4x4 inch embroidering area, does not have a built-in alignment method that uses fiducials like those found in the PCB and microfabrication industry. However, the user can position the design using buttons that move the needle in x,y in 0.5 mm increments. In our method, the sewing needle is moved to locate a pair of alignment marks on the part, which consist of a pair of laser-cut or 3D printed features 6 cm apart. The user loads a small test file and uses the machine's manual adjustments to move the needle over each alignment mark, lowering the needle to verify alignment. The Brother PE525 reports the current needle location to within 0.5 mm on its LCD screen. Users can often make a finer estimate by careful inspection. The user discards the small test file, and enters the measured coordinates of the left alignment mark (x_1, y_1) and right alignment mark (x_2, y_2) into MATLAB software to generate a translated and rotated stitch file containing the pattern to be stitched.

For a design file with alignment marks drawn at $(-x_0, 0)$ and $(+x_0, 0)$, the alignment software generates a new .exp file with each x,y stitch coordinate transformed as follows:

$$X_Center = (x_1 + x_2) / 2, \quad Y_Center = (y_1 + y_2) / 2 \quad (1)$$

$$Rotation_Angle = \tan^{-1}((y_2 - y_1) / (x_2 - x_1)) \quad (2)$$

$$\theta = \tan^{-1}(y/x) \quad (3)$$

$$r = \sqrt{x^2 + y^2} \quad (4)$$

$$x_{new} = r \cos(\theta + Rotation_Angle) + X_Center \quad (5)$$

$$y_{new} = r \sin(\theta + Rotation_Angle) + Y_Center \quad (6)$$

where x_{new}, y_{new} are the positions of each stitch coordinate in the modified design file.

The software calculates relative displacements between stitches and puts them into the binary .exp format. It also adds “jump” stitches to move the needle from the origin to the start of the design file, in the case that the distance is greater than the maximum encodable 12.7 mm displacement. At run-time, some machines (including the Brother PE525) ignore bounding-box information in the file header and instead, automatically center the data—potentially ruining the alignment. The rotation program avoids the auto-alignment problem by inserting a centered 9x9 cm bounding box at the same position every time. As long as the rotated and translated file does not escape this bounding box, the modified file will be correctly aligned when it is loaded and stitched on the still-aligned part with no user-entered offset or rotation on the machine.

The .exp format works with several brands of embroidery machines and viewing software, but not with the Brother PE525, which uses .pes format. Many file conversion programs are available, including the StitchBuddy program on iOS which converts files from .exp to .pes for this work.

Because accidental contact with a PCB or plastic part will break the needle, preparation of a new pattern usually includes stitching a test into a paper printout of the pattern to make sure that no stitches will run into a hard material. In this work, however, the materials were thin enough (0.125 mm polyester) that the needle could punch through. The main concern is making sure the pattern is aligned with the laser-cut edges over the entire 4x4 inch area, so the paper printout test is still worth carrying out.

Figure 1 shows a field of laser-cut frosted Mylar beams attached to a water-soluble sticky stabilizer (*Vilene Plus*) in an embroidery hoop. Because the beams are still attached to the original Mylar sheet at the left and right edge, they remain aligned to a pair of marks at the left and right of the middle beam in Figure 1a. Figure 1b shows the conductive thread on the back side. On top, there is insulating thread in the same pattern.

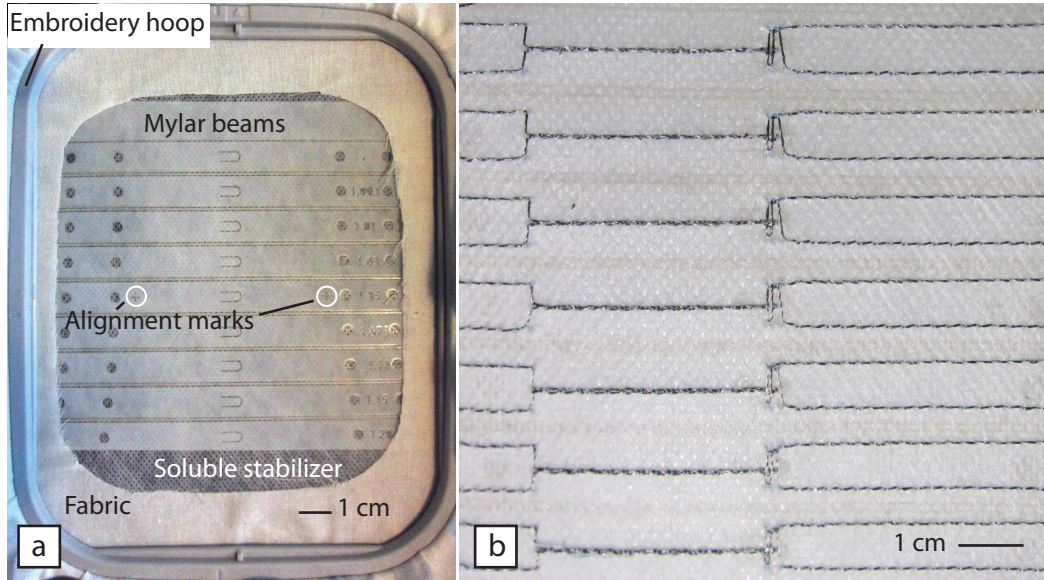


Figure 1. (a) Photo of a beam array ready for alignment. (b) Back side after aligning conductive thread pattern.

2.2 Buckling beam modeling

The conductive fiber-based switches in this paper are installed in the center of a bistable buckling beam to determine the beam's "up" or "down" binary state. The shape of the buckling beam is determined using the theory of thin-beam elastica. In these calculations, the Euler-Bernoulli moment-curvature relationship (Equation 7) is integrated to solve for x,y coordinates that match the boundary conditions at the ends of the beam:

$$M=EI d\theta/ds \tag{7}$$

where M is the bending moment at any section of the beam, ds is differential arclength, $d\theta$ is the differential change in beam inclination angle, I is the moment of inertia of the rectangular beam, and E is the modulus.

When the beam endpoints are horizontal, there are two symmetric states as seen in Figure 2a, but as the beam ends are rotated, the up- and down- shapes differ as illustrated in Figure 2b. The compressed beam's bistability is lost as the endpoints rotate beyond a critical angle. Interestingly, at the critical angle, the lower beam shape is self-similar to the upper one; for example the lower arc in Figure 2b can be constructed from six copies of the half-arc of the upper beam. This happens because at the critical angle, the inflection points replicate the same boundary conditions and beam compression ratio as the endpoints.

We previously explored the stability of these tensioned arcs using analytical [15] and finite element [16] modeling, and determined how the moments around the endpoints govern the state of the beam. This model showed that as long as the beam is thin (thickness \ll width) and can support itself, the compression ratio L/w is the chief factor in determining the critical angle. Bistable beams with the shapes in Figure 2 can therefore be achieved using a wide variety of construction materials and dimensions, including materials compatible with laser cut cantilevers and conductive thread contacts.

In this work, a cantilever is cut from the center of the beam making it have a smaller effective cross-section at the center. Its effect on the critical snap-through angle will be discussed alongside results.

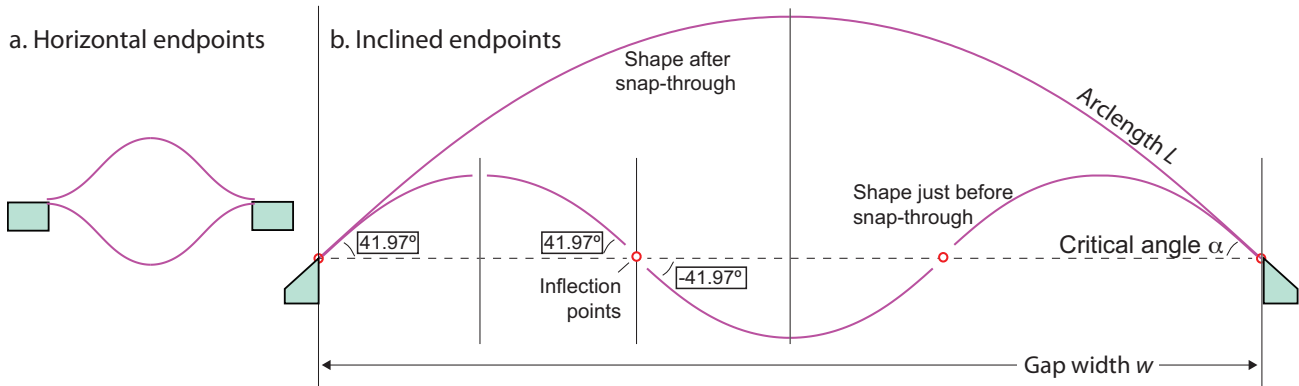


Figure 2: (a) A compressed beam with horizontal endpoints has two symmetric equal-energy states, “up” or “down.” (b) When the endpoints are no longer horizontal, the symmetry is broken. A beam with compression ratio (arclength L / gap width w) = 1.15 has two stable shapes at or below a critical angle of approximately 42 degrees; at greater angles only the upper arc is stable. The critical angle is a function of the beam compression ratio and does not depend strongly on material properties.

2.3 Design and fabrication of the bistable switch

The beam and cantilever were made from 0.005 inch (125 micron) thick frosted polyester (Mylar) film. The film was cut on a 40 Watt laser cutter (Epilog Mini) at 83% speed, 15% power and 2500 Hz settings. Alignment marks and labels were etched into the beam surface using raster settings of 86% speed, 32% power.

The cantilever was 5 mm long and 3 mm wide with a rounded tip. The amount of material lost by laser cutting (kerf) was approximately 0.3 mm, a little more than twice the material thickness; cantilevers did not touch the edges of the beam when it was bent back and forth during testing.

After cutting, but before separating the beams from the array, the design was transferred to the sticky side of the water-soluble stabilizer for embroidery alignment. The embroidery pattern used a 2 mm stitch length, except for the three strings suspended across the cantilever. A #10 (0.7 mm diameter) needle was able to punch through the beam without any problems. The top thread (needle thread) was insulating polyester embroidery thread, while the bottom thread (bobbin thread) was conductive silver-plated nylon (117/17 2 ply, PlugandWear product PW018).

Figure 3a shows a schematic of the beam cutout without and with conductive thread, and Figure 3b is a close-up image of three beams after release from the stabilizer. Three strings with a 1mm separation were suspended across the cantilever to make contact with a conductive thread that had been sewn earlier in the pattern. In Figure 3b, the middle of the three suspended threads can be seen making the most contact with the threads on the cantilever.

Because the polyester thread spanning the cantilever will constrain the motion of the cantilever away from the conductive thread and possibly interfere with switch opening, it was cut after applying glue (E-6000 Permanent Craft Adhesive) to the ends of the conductive thread to hold it in place. Finally, the soluble stabilizer was removed by soaking in hot water for 5 minutes, and individual beams were separated for testing.

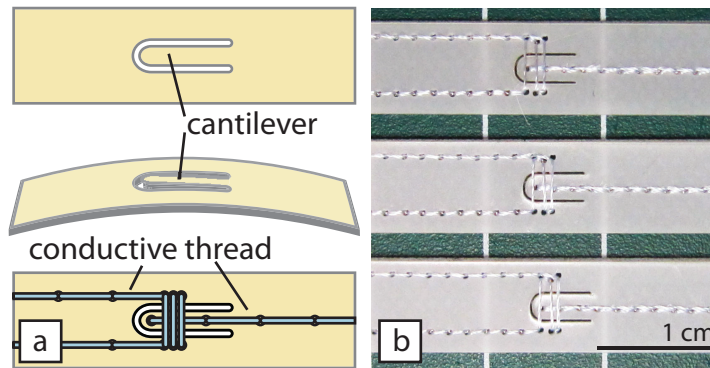


Figure 3: (a) Schematic of laser-cut cantilever. Center image shows the cantilever deflecting above the surface of the bent beam. (b) Close-up image of released beams showing three suspended threads across each cantilever.

2.4 Testing Apparatus

All critical-angle tests were carried out using an apparatus that kept the beam symmetric about the center using meshed laser-cut acrylic gears (Figure 4). Beams of different compression ratios (L/w) were installed in clamps, and the switch contacts were connected to an analog-to-digital converter input with a $10\text{ k}\Omega$ pull-up resistor.

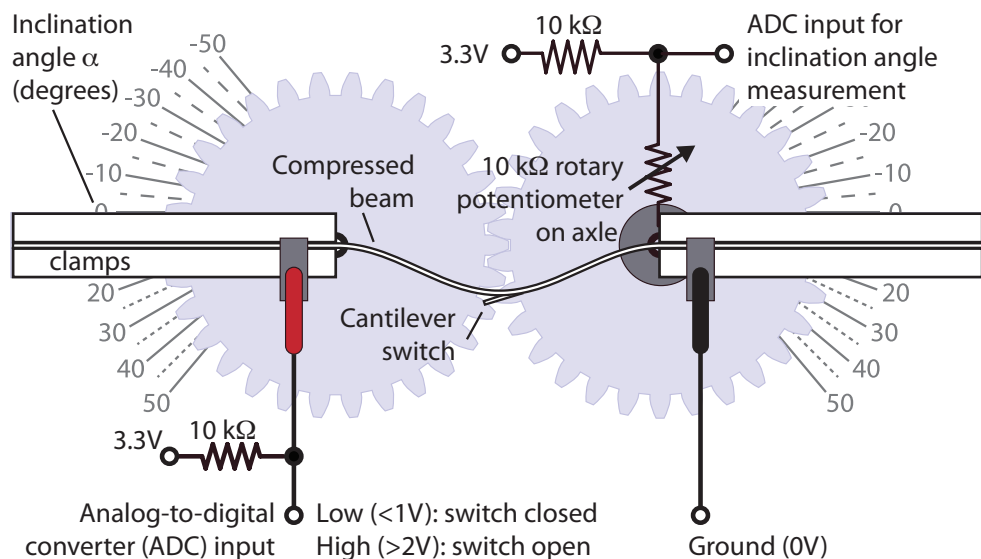


Figure 4: Testing apparatus to measure both the electrical state of the beam, and the inclination angle of the beam endpoints. One end point is rotated by hand while data are recorded to two computer inputs.

To keep track of the angle, a $10\text{ k}\Omega$ rotary potentiometer was installed on one of the gear axles and connected to another digital input with $10\text{ k}\Omega$ pull-up resistor. The angle increments were measured as one of the beam ends was moved by

hand, and the recorded voltage was correlated with angle. Later, this calibration was used in a lookup table to determine the inclination angle from the voltage measured during experiments. Signals were recorded at 100 Hz using an Arduino microcontroller board to communicate the two voltage readings to serial terminal software (CoolTerm).

3. RESULTS

Beams with compression ratios ranging between 1.01 and 1.10 were tested in the angle measurement setup of Figure 4. The compression ratio L/w is always greater than 1, describing how much excess beam spans the 5 cm gap between the two axles. Figure 5 shows the two signals received from experiments on the longest beam with compression ratio 1.1. This 5.5 cm beam had a 10% surplus length. The beam would snap through to the “up” state if the inclination angle (indicated by the position of the top of the clamps in Figure 4) were greater than approximately 41.2 degrees. The “up” state corresponded to a closed switch, 0V signal for the beam orientation used in these experiments. It would snap through to the “down” state (open switch, 3.3 V signal) at inclination angles less than approximately -31.7 degrees.

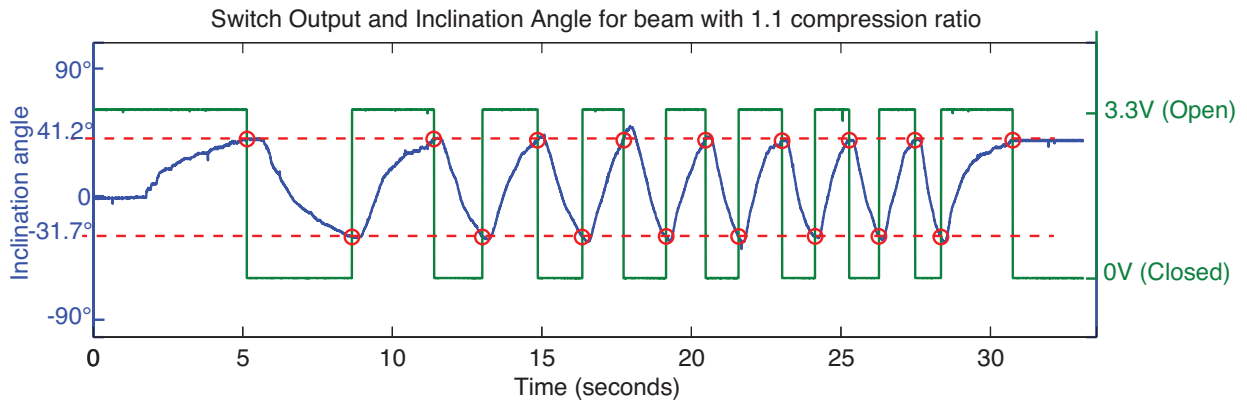


Figure 5: Inclination angle data and switch state data for a beam with 10% surplus length (1.1 compression ratio)

Five beams of different lengths were tested for comparison with the calculated snap-through angle as a function of surplus beam length. Figure 6 shows the results, with uncertainties coming from the standard deviation of the angle measured at all switch transition events in the file. For a given beam, the snap-through angle was consistently within 5% or better of its average value.

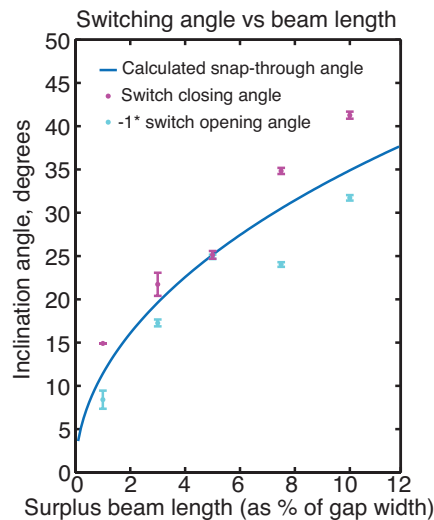


Figure 6: Positive and negative switching angles overlaid on the calculated snap-through angle as a function of beam length.

All of the beams except for the 5.25 cm (5% excess length) beam had significantly different values for the absolute value of their positive vs negative snap-through angle, with the magnitude of the negative switch-opening angle smaller than the positive switch-closing angle. Aside from this discrepancy, the beams generally followed the calculated snap-through curve, even though the cantilever cutout meant that the beam did not have the constant rectangular cross-section assumed in the model.

4. DISCUSSION

In Figure 6, the critical switching angle was seen to depend on surplus beam length in a manner consistent with calculations for the snap-through angle. In between the two critical angles (red dotted lines in Figure 5), there was hysteresis: the switches were bistable, meaning they could be open or closed, with their state depending on the previous state of the beam. If the history was not known, the switches worked as a threshold angle detector with a “negative” interpretation: if the signal was 0, the 5.5 cm beam of Figure 5 could not be at an inclination angle less than -31.7 degrees, and if the signal was high, the angle could not be greater than 41.2 degrees.

The observation that the beam usually “hangs on” longer when making the down to up transition, than the up to down, could be related to the asymmetry in mechanical contact between the conductive threads on the cantilever side vs the lack of constraints on the other side where the insulating threads had been cut. For a given beam, the exact switching angle depends on the microscopic geometry around the cantilever and conductive thread pattern.

5. CONCLUSIONS AND FUTURE WORK

For an individual structure, the switching threshold value was consistent enough to use as an angle limit sensor, with threshold angle value set by the surplus beam length. Such switches would also be a good match to a system where the goal is simply to detect whether a structure is in one of two positions.

Previously, we developed a fast method to make arbitrary shapes from collections of binary arcs. The method applies the error-diffusion dithering technique from computer graphics to match the local curvature, and is thousands of times faster than simulated annealing [17]. In future work, we will expand on this result to move the array from an initial to final shape without self-intersection, using a minimal number of energy-consuming snap-through events. Flexible integrated switches will provide shape verification in environments where obstacles may prevent snap-through. Sensing is also essential to power minimization because the signal will tell actuators to stop drawing current immediately after snap-through occurs. Figure 7 shows our previous experimental work on sensor chains made from bistable arcs equipped with switches [18,19]. The surface mount switches were designed for rigid PCBs and de-bonded from the flex circuit after several cycles. This problem motivated the conductive fiber-based switches in this paper.

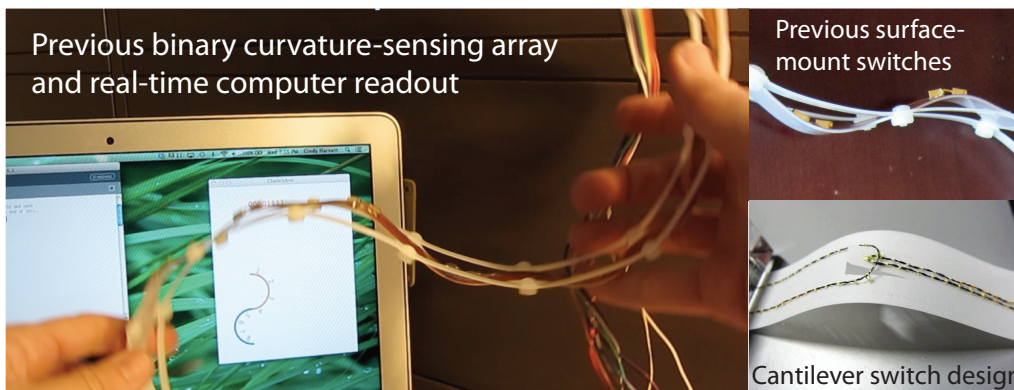


Figure 7: Implementation of a shape sensor from a series of 8 bistable arcs that report their state to a computer (video in [19]). The cantilever switches in this work will replace the surface-mount switches shown at left and top right.

Two general application cases are envisioned for this cantilever structure: inserting a switch into an existing flexible circuit to detect whether a joint is at its maximum or minimum angle, and using the digital switch to detect the state of a binary actuator. Applications in robotics could include “digital robotics” and built-in limit switches inside flexible circuit routing paths.

REFERENCES

- [1] Rogers, J. A., Someya, T., and Huang, Y., "Materials and mechanics for stretchable electronics," *Science* 327(5973), 1603-1607 (2010).
- [2] Palleau, E., Reece, S., Desai, S. C., Smith, M. E., and Dickey, M. D., "Self-Healing Stretchable Wires for Reconfigurable Circuit Wiring and 3D Microfluidics," *Advanced Materials* 25(11), 1589-1592 (2013).
- [3] Hirsch, A., Michaud, H. O., Gerratt, A. P., De Mulatier, S., and Lacour, S. P., "Intrinsically Stretchable Biphasic (Solid-Liquid) Thin Metal Films," *Advanced Materials*, doi:10.1002/adma.201506234 (2016).
- [4] Kramer, R. K., Majidi, C., Sahai, R., and Wood, R. J., "Soft curvature sensors for joint angle proprioception," In *Intelligent Robots and Systems (IROS)*, 2011 IEEE/RSJ International Conference on, 1919-1926 (2011).
- [5] Bilodeau, A., R., White, E. L., and Kramer, R. K., "Monolithic fabrication of sensors and actuators in a soft robotic gripper," In *Intelligent Robots and Systems (IROS)*, 2015 IEEE/RSJ International Conference on, 2324-2329 (2015).
- [6] Jost, K., Durkin, D. P., Haverhals, L. M., Brown, E. K., Langenstein, M., De Long, H. C., Trulove, P. C., Gogotsi, Y., and Dion, G., "Natural fiber welded electrode yarns for knittable textile supercapacitors," *Advanced Energy Materials* 5:1401286. doi: 10.1002/aenm.201401286 (2015).
- [7] Zhu, S., Ju-Hee, S., Mays, R., Desai, S., Barnes, W. R., Pourdeyhimi, B., and Dickey, M. D., "Ultrastretchable fibers with metallic conductivity using a liquid metal alloy core," *Advanced Functional Materials* 23(18), 2308-2314 (2013).
- [8] Kiourti, A., and Volakis, J. L., "High-geometrical-accuracy embroidery process for textile antennas with fine details," *IEEE Antennas and Wireless Propagation Letters* 14, 1474-1477 (2015).
- [9] Xu, S., Zhang, Y., Cho, J., Lee, J., Huang, X., Jia, L., Fan, J. A. et al. "Stretchable batteries with self-similar serpentine interconnects and integrated wireless recharging systems," *Nature Communications* 4, 1543 (2013).
- [10] Webb, R. C., Bonifas, A. P., Behnaz, A., Zhang, Y., Yu, K. J., Cheng, H., Shi, M. et al. "Ultrathin conformal devices for precise and continuous thermal characterization of human skin," *Nature Materials* 12(10), 938-944 (2013).
- [11] Lee, S., Reuveny, A., Reeder, J., Lee, S., Jin, H., Liu, Q., Yokota, T., et al. "A transparent bending-insensitive pressure sensor," *Nature Nanotechnology* 11, 472-478 (2016).
- [12] Kaltenbrunner, M., Sekitani, T., Reeder, J., Yokota, T., Kuribara, K., Tokuhara, T., Drack, M., et al. "An ultralightweight design for imperceptible plastic electronics," *Nature* 499(7459), 458-463 (2013).
- [13] Larson, C., Peele, B., Li, S., Robinson, S., Totaro, M., Beccai, L., Mazzolai, B., and Shepherd, R., "Highly stretchable electroluminescent skin for optical signaling and tactile sensing," *Science* 351 (6277), 1071-1074 (2016).
- [14] Saari, M., Cox, B., Galla, M., Krueger, P. S., Richer, E. and Cohen, A. L. "Multi-material additive manufacturing of robot components with integrated sensor arrays," In *Proc. of SPIE* 9494, 949404-1 (2015).
- [15] Beharic, J., Lucas, T. M., and Harnett, C. K., "Analysis of a compressed bistable buckled beam on a flexible support." *Journal of Applied Mechanics* 81 (8) 081011 (2014).
- [16] Bradshaw, R., Beharic, J., and Harnett, C. K., "Experimental Study and Numerical Analysis of Bistable Buckled Inclined Beams." *Proc, SEM Conference on Experimental and Applied Mechanics*, paper 481 (2014).
- [17] Harnett, C. K., and Kimmer C. J., "Digital Origami from Geometrically Frustrated Tiles." *Proc ASME IDETC Conference*, pp. V06BT07A046-V06BT07A046 (2013). Slides <http://bit.ly/1Sc4UXR>
- [18] Harnett, C. K. "Flexible Switching Sensors for Passive Shape Monitoring." presented at the International Society of Automation Passive Wireless Sensor Workshop, Washington, D. C., May 21 (2013).
- [19] Harnett, C. K., "Shape sensor demonstration video" <https://youtu.be/PfGDJjBC-Hw> (2013).